Tohoku J. Exp. Med., 2021, **255**, 135-142

Acceleration of Fracture Healing in Mouse Tibiae Using Intramedullary Nails Composed of β-Type TiNbSn Alloy with Low Young's Modulus

Yu Mori,[1] Hirokazu Fujisawa,[1] Masayuki Kamimura,[1] Atsushi Kogure,[1] Hidetatsu Tanaka,[1] Naoko Mori,[2] Naoya Masahashi[3] and Toshimi Aizawa[1]

[1]Department of Orthopaedic Surgery, Tohoku University Graduate School of Medicine, Sendai, Miyagi, Japan
[2]Department of Diagnostic Radiology, Tohoku University Graduate School of Medicine, Sendai, Miyagi, Japan
[3]Institute for Material Research, Tohoku University, Sendai, Miyagi, Japan

The optimal Young's modulus of material of orthopedic devices for fracture treatment is still unknown. The purpose of present study was to evaluate the impacts of intramedullary nails composed of a titanium alloy with low Young's modulus, on accelerating fracture healing compared with stainless steel with high Young's modulus. A β-type TiNbSn alloy with a low Young's modulus close to that of human cortical bone was developed for clinical application. TiNbSn alloy with a Young's modulus of 45 GPa and stainless steel with a Young's modulus of 205 GPa were compared, with respect to the impacts on fracture healing. Fracture and fixation using intramedullary nail were performed on the right tibiae of C57BL/6 mice. The assessment of bone healing was performed via micro-computed tomography, histomorphometry, and quantitative reverse transcription polymerase chain reaction. In micro-computed tomography, larger bone volumes were observed in the fracture callus treated with TiNbSn alloy in comparison with those treated with stainless steel. Histological assessments confirmed accelerated cartilage absorption and new bone formation in the TiNbSn alloy group compared with the stainless steel group. The expression of *Col1a1*, *Runx2, Dkk1*, and *Acp5* was higher in the TiNbSn alloy group, while that of *Col2a1* and *Col10a1* was lower in the late phase. The present study demonstrated that the fixation by intramedullary nails with TiNbSn alloy offered an accelerated fracture healing with promotion of bone formation via increased *Runx2* expression. TiNbSn alloy might be a promising material for fracture treatment devices.

Keywords: bone formation; bone remodeling; fracture healing; low Young's modulus; TiNbSn alloy
Tohoku J. Exp. Med., 2021 October, **255** (2), 135-142.

Introduction

Stainless steel together with titanium alloys are widely used in orthopedic implants for fractures as biomedical materials (Long 2008). Especially, titanium alloys are generally preferred for orthopedic applications because of their excellent biocompatibility and corrosion resistance (Uhthoff et al. 1981; Khan et al. 1999; Rack and Qazi 2006; Cui et al. 2011). Ti6Al4V alloy, the commonly used biomedical titanium alloy, has a lower Young's modulus (110 GPa) than that of stainless steel (205 GPa) (Long and Rack 1998). However, the Young's modulus of Ti6Al4V is still much higher than that of human cortical bone (11-20 GPa) (Bayraktar et al. 2004). The divergence in Young's modulus between the cortical bone and biomedical materials evokes stress shielding by inhibiting weight-bearing transmission (Maistrelli et al. 1991; Huiskes et al. 1992; Glassman et al. 2006). Fracture fixation devices with excessive rigidity were reported to lead poor results, such as suppressed callus formation, delayed fracture healing and non-union (Molster et al. 1982, 1983; Henderson et al. 2011; Ebraheim et al. 2013). In contrast, the previous studies demonstrated that intramedullary nails of titanium alloy with low Young's moduli have indicated enhanced fracture healing in terms of bone strength after fracture union and imaging studies, and these functional materials could prevent bone atrophy due to stress shielding (Sha et al. 2009; Niinomi and Nakai 2011).

Received July 7, 2021; revised and accepted August 2, 2021. Published online October 16, 2021; doi: 10.1620/tjem.255.135.
Correspondence: Yu Mori, Department of Orthopaedic Surgery, Tohoku University Graduate School of Medicine, 1-1 Seiryo-machi, Aoba-ku, Sendai, Miyagi 980-8574, Japan.
e-mail: yu-mori@med.tohoku.ac.jp

To resolve these negative effects of Ti6Al4V alloy on bone, a new β-type TiNbSn alloy with a lower Young's modulus of nearly 40 GPa was developed (Matsumoto et al. 2005; Miura et al. 2011). This TiNbSn alloy also has greater tensile strength, compared with Ti6Al4V alloy via heat treatment (Jung et al. 2013). Furthermore, TiNbSn alloy showed excellent biocompatibility, similar to that of Ti6Al4V alloy when inserted into the medullary canals of rabbits femurs as rods, similarly with reduced cytotoxicity in the osteoblasts culture tests on the TiNbSn alloy discs (Miura et al. 2011). TiNbSn alloy anodized with acetic acid and sulfuric acid also showed greater abilities for the formation of hydroxy apatite, strong bone connection, and superior osseointegration (Tanaka et al. 2016; Masahashi et al. 2017; Kunii et al. 2019; Masahashi et al. 2019). In contrast, TiNbSn alloy anodized with sodium tartrate exhibited superior photoactivity under ultraviolet light irradiation, which might be useful for antibacterial activity (Masahashi et al. 2021). The stiffness and Young's modulus of TiNbSn alloy gradually increased by heat treatment at temperatures above 423 K, and TiNbSn alloy was demonstrated as a functionally graded material (Hanada et al. 2014). In animal experimental models of rabbit tibia osteotomy and murine tibia fracture using intramedullary nails made of TiNbSn alloy, these nails were shown to be more effective in promoting bone healing than the Ti6Al4V alloy and TiNbSb alloy, whose Young's moduli are increased upon heating (Fujisawa et al. 2018; Kogure et al. 2019). However, no comparative study has been done on the process of bone healing when there is a large difference in Young's moduli of intramedullary nails such as between TiNbSn alloy and stainless steel. By comparing materials with such a large difference in Young's modulus, the authors considered the possibility of clarifying the molecular biological mechanism of the effect of the difference in Young's modulus on fracture treatment.

The aim of the present study was to determine the effect of the elastic modulus of intramedullary nails on fracture healing. To assess this, the impacts of TiNbSn alloy and stainless steel intramedullary nails on bone healing were investigated. Radiological, histological, and molecular biological assessments were performed to clarify the modulus-dependent effects of TiNbSn alloy and stainless steel on bone healing behavior.

Materials and Methods

Preparation of the wire of TiNbSn alloy

The composition of the TiNbSn alloy ingot was Ti-25.4% Nb-9.9% Sn (mass; %), TiNbSn alloy rod was fabricated from ingot by extrusion and swaging. The rod was drawn into a thin wire with a diameter of 0.4 mm. The details of preparation of TiNbSn alloy wire were described in the literature (Fujisawa et al. 2018). The Young's modulus of the drawn wire was measured using the free resonance vibration method (45 GPa).

Animals

C57BL/6 mice were purchased from Charles River, Japan (Tokyo, Japan). All mice were housed in the Animal Experiments Facilities of Tohoku University, which is an environmentally controlled and specific pathogen-free facility. The animal experiment protocol was reviewed and approved by the Animal Studies Committee of Tohoku University (2014-MdA245). 12-week-old male mice were used for all experiments in the present study.

Surgical procedure

The surgical procedures were performed under inhalation anesthesia with 2% isoflurane (Forane; Abbott, Wiesbaden, Germany). The standardized closed transverse fractures were created in the tibial diaphysis using a fracture device, followed by intramedullary insertion of the TiNbSn alloy and stainless steel (SUS304: Natsume Manufacturing, Tokyo, Japan) wires (Young's modulus, 45 and 205 GPa, respectively) into the right tibiae, as previously described (Kamimura et al. 2015; Mori et al. 2016). The wires with 0.4 mm in a diameter and 17 mm in a length were used as intramedullary nails. This fracture device worked by a blunted guillotine driven by dropping a 230 gram weight from a height of 17 cm. All mice with surgical procedure were allowed to move freely in their cages immediately after surgery. The mice were euthanized in a carbon dioxide gas chamber at 7-28 days after surgery. After the euthanasia, the tibia was detached from the overlying skin and femur, leaving the surrounding muscles intact.

Micro-computed tomography (Micro-CT)

The harvested tibiae for micro-CT analyses were stored in 70% ethanol at 4°C. Micro-CT imaging was done 14 days after fracture. Micro-CT analyses were performed using a micro-CT scanner (Scan Xmate-L090; Comscan Techno Co. Ltd., Yokohama, Japan) operating at a peak voltage of 75 kV and 100 μA. The scanned area were 253 images of proximal and distal to the fracture line at a resolution of 10.4 μm per voxel, and the resolution of images was 516 × 506 pixels. The parameters including total volume (TV; mm^2), bone volume (BV; mm^2), bone volume ratio (BV/TV; %), and percentage of new cortical shell area (new cortical shell area/total volume; %) were evaluated and calculated at the axial slice with the maximal cross-sectional area of the callus, using image analysis software (ImageJ version 1.50), as described previously (n = 6 per group) (Kamimura et al. 2015).

Histological analysis

The tibiae were fixed through immersion in 4% paraformaldehyde for 48 hours and then transferred to 30% sucrose in 0.1 M phosphate-buffered saline (pH 7.4) for 24 hours. Histological analyses were performed at 7, 10, and 14 days after fracture. The intramedullary nails were removed before embedding the specimen for histological

analysis. The tissues were positioned in embedding medium for the frozen tissue specimen (Tissue-Tec; Sakura Finetek, Torrance, CA, USA), stored at −80°C until they were sectioned. Sagittal cryosections (thickness, 7 μm) of undecalcified fracture calluses were prepared with use of a cryostat (Bright, Huntingdon, UK) with a disposable microtome blade (S35 Fine; Feather Safety Razor, Osaka, Japan) using a tape transfer method (Cryofilm Type IIC; Sectionlab, Hiroshima, Japan). The details of the tape transfer method were described in the previous report (Mori et al. 2016). Tissue sections those were attached to the tape were placed on a glass slide with the specimen side up. The sections were individually stained with Alcian blue, hematoxylin and eosin. Cartilage tissue and newly formed bone were measured using ImageJ software (version 1.53) according to the American Society for Bone and Mineral Research guidelines (Dempster et al. 2013). The sections after staining were examined and photographed using an Olympus BX51 microscope with a DP73 digital camera (Olympus, Tokyo, Japan) and analyzed using CellSens software (Olympus).

Quantitative reverse transcription polymerase chain reaction (RT-PCR)

The callus specimens were harvested at 7, 10, and 14 days after surgery. Callus specimens were collected from six mice in each group on days 7, 10, and 14, for a total of 36 mice in both groups were used for the RT-PCR analysis. Muscles and original bone were separated from the calluses. Quantitative RT-PCR was performed as previously described (Izumiyama et al. 2019). The extraction of total RNA was performed using TRIzol (Invitrogen Corp., Carlsbad, CA, USA) and RNeasy Mini Kit (Qiagen, Hilden, Germany). Synthesis of cDNA from the total RNA was performed using cDNA reverse transcription kit (Applied Biosystems, Foster City, CA, USA). Real-time amplification of the target genes was performed using Taqman Universal Master Mix II with Uracil-N glycosylase and ready-to-use Taqman Gene Expression Assays (Applied Biosystems) for collagens (*Col1a1*, Mm00801666_g1; *Col2a1*, Mm01309565_m1; *Col10a1*, Mm00487241_m1), runt-related transcription factor 2 (*Runx2,* Mm00501584_m1), dickkopf-related protein 1 (*Dkk1*, Mm00438422_m1), acid phosphatase 5 tartrate resistant (*Acp5*, Mm00475698_m1), and Glyceraldehyde-3-phosphate dehydrogenase (*Gapdh*, Mm99999915_g1) as an endogenous control. Relative gene expression data were calculated using the delta-delta-Ct method with PCR-efficiency correction using StepOne software (version 2.2.2; Applied Biosystems).

Statistical analysis

Statistical analyses were performed using JMP software version 16 (SAS, Cary, NC, USA). All data are expressed as the mean ± standard deviation (SD). The statistical significance of the differences between values was evaluated using Student's *t*-test and one-way analysis of variance with the Tukey-Kramer test. Value of $P < 0.05$ was regarded as statistically significant.

Results

Radiographic findings

Fig. 1 shows representative radiographic images of the fracture model. All fractured tibiae healed without non-union and nail failure. A cartilage callus formation started at 7 days after fracture, and a bony callus was detected until 14 days after fracture. A new bony cortical shell around the callus was established until 21 days after fracture in both groups. On day 28, the fracture healing and bone remodeling process were completed in both groups.

Micro-CT analysis

Micro-CT images of calluses harvested at day 14 showed the formation of calcified bony callus around the fracture site in both groups. The TiNbSn alloy group showed increased density in the calcified callus area in comparison with the stainless steel group (Fig. 2). The quantitative analyses of the structure of fracture calluses are shown in Fig. 3. There was no significant difference in the TV between the groups. In contrast, BV was significantly higher in the TiNbSn alloy group than in the stainless steel group ($P < 0.001$). There was a significant difference in BV/TV between the groups ($P < 0.001$). Furthermore, there was a significant difference in the outer cortical shell formation between the groups on 14 days after fracture ($P < 0.001$) (Fig. 3).

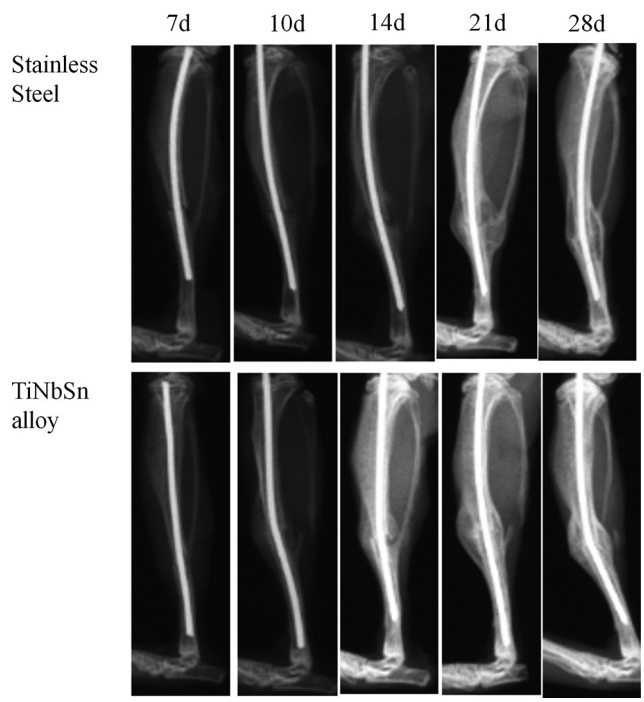

Fig. 1. Representative radiographic images of fractured tibiae during fracture healing in the stainless steel and TiNbSn alloy groups.
There were no cases with non-union and implant failure.

Histological analysis

The area stained with Alcian blue indicated cartilaginous tissue in the fracture callus. The trend of tissue repair and remodeling showed that cartilaginous absorption and bone formation proceeded from the periphery to the center of the callus in both groups. On day 7, cartilaginous tissue occupied the most of calluses, demonstrating positive Alcian blue staining in both groups. The TiNbSn alloy group showed an advanced peripheral new bone formation compared to the stainless steel group (Fig. 4). At days 10 and 14, new bone formation at the peripheral area of callus (arrows) and absorption of the cartilaginous tissue (stars) were proceeded in the TiNbSn alloy group compared with the stainless steel group. On day 14, most of the fracture calluses in the TiNbSn group were replaced by newly formed bone from the cartilaginous tissue.

Quantitative histomorphometric analyses were performed to assess the differences between the groups in fracture callus. No significant differences in the total volume of callus area between the groups were observed on days 7, 10, and 14 (Fig. 5A). The cartilaginous area significantly decreased with time on days 7, 10, and 14 in the TiNbSn alloy group (day 7 vs. day 10, $P = 0.037$; day 10 vs. day 14, $P = 0.015$). Furthermore, there was a significant difference between the two groups on day 14 ($P = 0.013$) (Fig. 5B). The area of newly formed bone increased significantly with time on days 7, 10, and 14 and was significantly larger in the TiNbSn alloy group than in the stainless steel group on days 7, 10, and 14 ($P = 0.041$, $P < 0.001$, and $P < 0.001$, respectively) (Fig. 5C).

RT-PCR analysis

The results of quantitative RT-PCR analyses for the expression of *Col1a1*, *Runx2, Col2a1*, *Col10a1*, *Dkk1*, and *Acp5* are shown in Fig. 6. Expression of the osteogenic gene *Col1a1* increased progressively until day 14 in both groups, especially with a significant difference in the TiNbSn alloy group (day 7 vs. day 10, $P = 0.023$; day 10 vs. day 14, $P = 0.016$). Furthermore, there was a significant difference between the two groups on day 14 ($P = 0.029$) (Fig. 6A). Likewise with *Col1a1*, the expression of *Runx2* was elevated over time until 14 days after fracture with a significant difference in the TiNbSn alloy group (day 7 vs. day 10, $P = 0.017$; day 10 vs. day 14, $P = 0.022$). There were significant differences between the two groups on day 10 and 14 ($P = 0.032$ and $P = 0.028$) (Fig. 6B). The expression of the chondrogenic gene *Col2a1* was significantly decreased in the TiNbSn alloy group on day 14 ($P < 0.001$), with a significant difference in expression between the groups on day 14 ($P = 0.011$) (Fig. 6C). There was a significant difference in the expression of *Col10a1* on day 14 between the groups ($P = 0.039$) (Fig. 6D). The expression of *Dkk1* was increased until day 14 in both groups, with a significant difference in the TiNbSn alloy group (day 10 vs. day 14, $P < 0.001$), in addition to a significant difference between the two groups on day 14 ($P = 0.011$) (Fig. 6E).

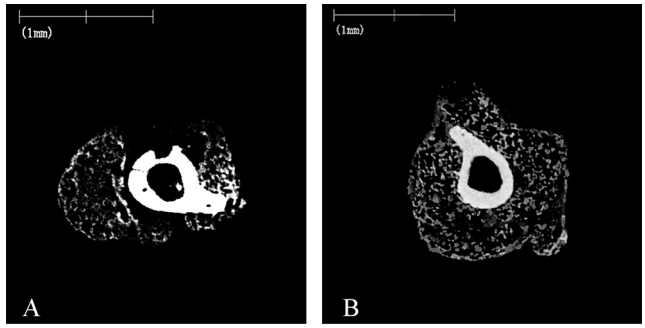

Fig. 2. Micro-CT images of the fracture callus in the stainless steel and TiNbSn alloy groups at 14 days after fracture. Representative axial image of the fracture callus in the stainless steel group (A) and the TiNbSn group (B).

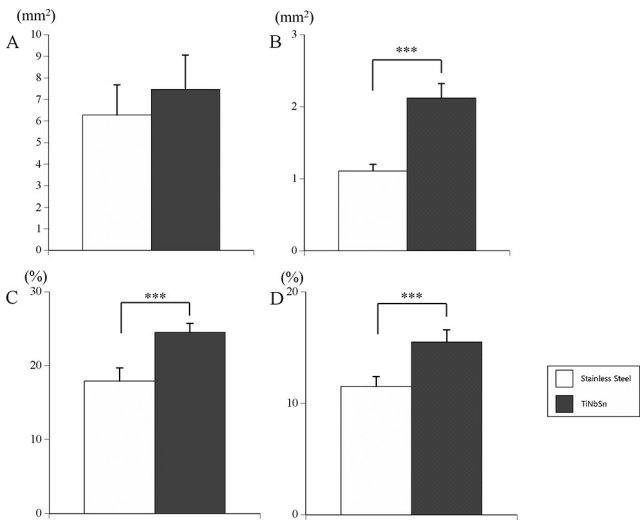

Fig. 3. Quantitative structural analyses of the fracture calluses in micro-CT images.
(A) Total volume of fracture callus. (B) Bone volume of fracture callus. (C) Ratio of bone volume to total volume. (D) Ratio of formatted outer cortical shell in the fracture callus. Results are expressed as the mean ± SD ($n = 6$). ***$P < 0.001$ using Student's *t*-test.

Expression of the osteoclastic gene *Acp5* significantly increased progressively in both groups until day 14 (stainless steel group, day 10 vs. day 14, $P < 0.001$; TiNbSn alloy group, day 10 vs. day 14, $P < 0.001$) and was significantly higher in the TiNbSn group than in the stainless steel group on day 14 ($P = 0.017$) (Fig. 6F).

Discussion

In this study, the impacts of Young's modulus on the mechanical property in intramedullary nails fixation during fracture healing was investigated by comparing the effects of TiNbSn alloy and stainless steel, which had a large Young's modulus difference. In TiNbSn alloy group, the results of micro-CT, histomorphometric, and RT-PCR analyses demonstrated facilitated cartilaginous tissue replacement and new bone formation at the fracture callus in comparison with the stainless steel group. The low Young's

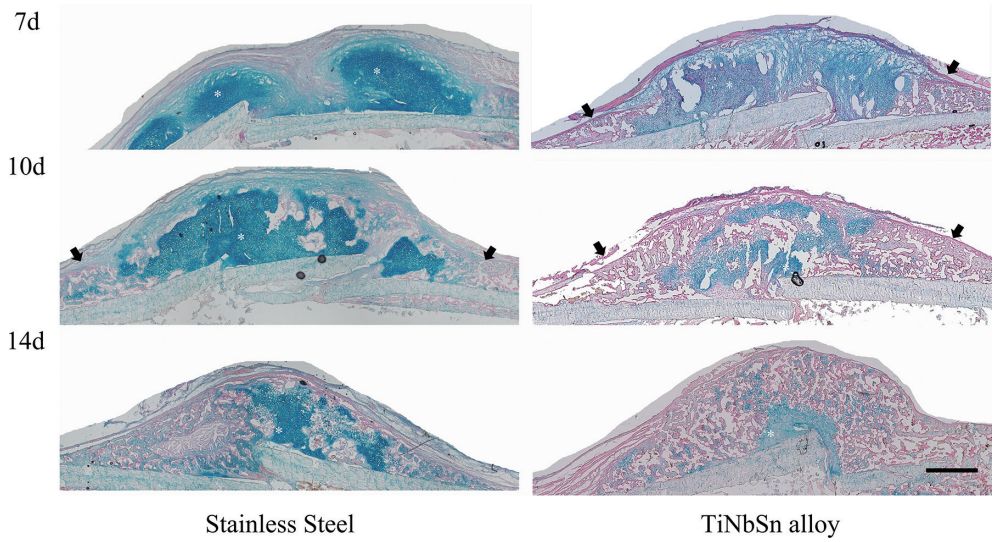

Fig. 4. Representative histological images of fracture healing.
Stars, Alcian blue-stained area indicating cartilaginous tissue; arrows, new bone formation area.
Scale bar = 500 μm

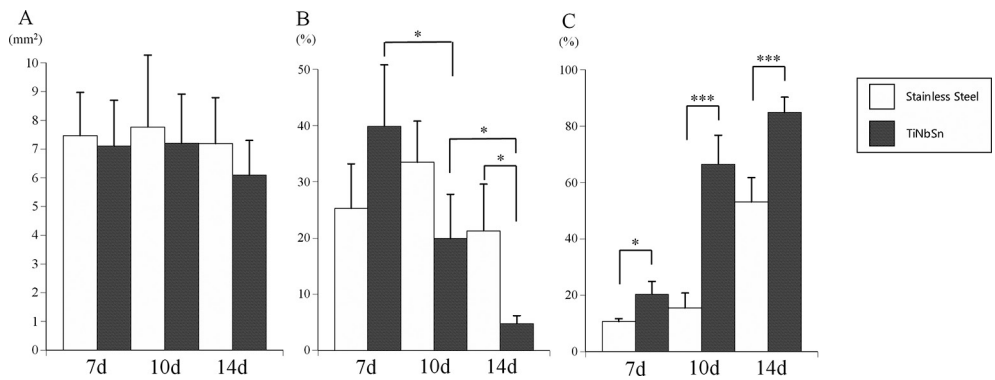

Fig. 5. Quantitative analysis of the histological images of the fracture calluses.
(A) Total volume of fracture callus. (B) Ratio of cartilaginous tissue volume. (C) Ratio of bone tissue volume. Results are expressed as the mean ± SD (n = 6). *P < 0.05, ***P < 0.001 using one-way analysis of variance with the Tukey-Kramer test.

modulus of TiNbSn alloy could promote fracture healing by increased bone formation due to the enhancement of osteogenesis by promoting Runx2 expression in the fracture callus.

The results of micro-CT and histomorphometric analyses demonstrated that the differences in the Young's modulus of the nails did not affect the total volume of callus, even in a comparison using materials with large differences in Young's modulus. The difference in Young's modulus was not related to the volume of the callus, but had an effect on the amount of bone formation. These results demonstrated the increase in new bone formation at the callus treated with the TiNbSn alloy, and were consistent with those of previous study (Fujisawa et al. 2018). The motion between bone fragments was considered to affect callus formation and fracture healing (Claes et al. 1997; Utvag and Reikeras 1998; Utvag et al. 1999; Augat et al. 2003), with axial interfragmentary motion exerting positive effects on bone healing. Adequate motion between bone fragments could contribute to accelerate callus maturation and produces mechanical strength. In the comparison between TiNbSn alloy (45 Gpa) and stainless steel (205 GPa), the greater difference in the formation of new bone within the callus than between untreated (45 Gpa) and heated TiNbSn alloy (78 GPa) was speculated to be due to the difference in Young's modulus. There were reports showing that fracture treatment plates made of Ti29Nb13Ta4.6Zr with a low Young's modulus tended to promote bone healing, although quantitative evaluation had not been performed (Sumitomo et al. 2008; Niinomi and Nakai 2011). The authors considered these reports to be consistent with the results of the present study using intramedullary nails made of TiNbSn alloy. Together, these findings indicate that TiNbSn alloy nails have adequate elastic characteristics, and their reduced Young's moduli seem to provide adequate motion between bone fragments and accelerated fracture healing. However,

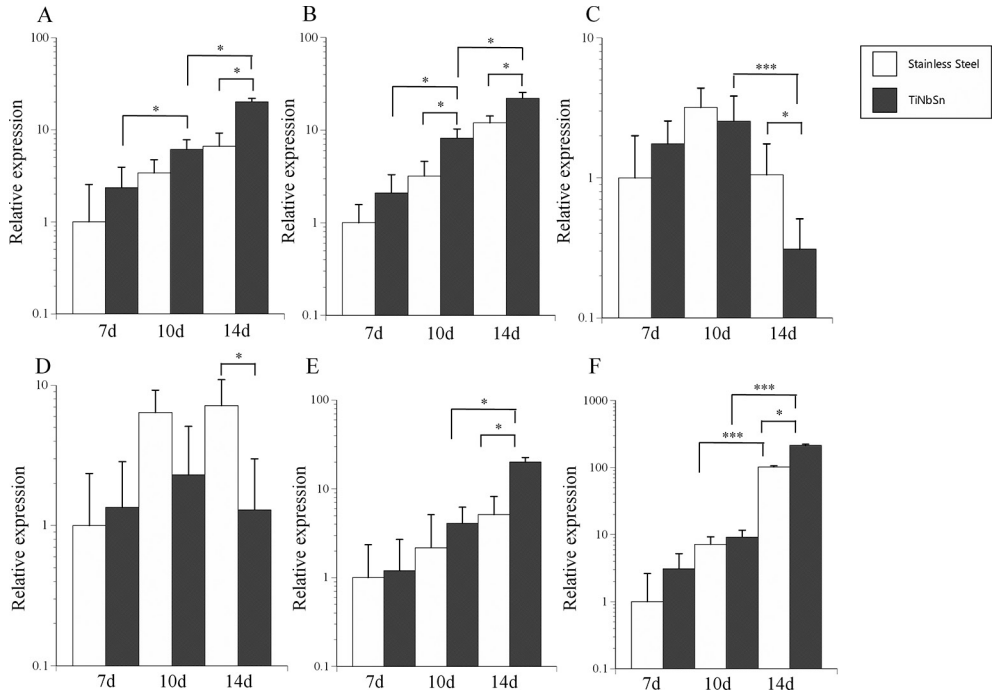

Fig. 6. Quantitative analyses of mRNA expressions of chondrogenic, osteogenic, and osteoclastic genes.
(A) *Col1a1*, (B) *Runx2,* (C) *Col2a1*, (D) *Col10a1*, (E) *Dkk1*, and (F) *Acp5*. Results are expressed as the mean ± SD (n = 6). **P* < 0.05, ****P* < 0.001 by one-way analysis of variance with Tukey-Kramer test.
Col, collagen; Runx2*,* runt-related transcription factor 2; Dkk1, dickkopf-related protein 1; Acp5, acid phosphatase 5, tartrate resistant.

the optimal Young's moduli might differ among different types of experimental models and orthopedic devices. The effect of accelerated bone healing with TiNbSn alloy plates in a rabbit tibial osteotomy model was also tested in another experiment.

It is still unclear how fracture healing will improve after fixation with a low Young's modulus orthopedic titanium alloy implants. A small number of studies have evaluated the relation between material property and changes in molecular expressions during fracture healing. The less rigid fixation methods promoted chondrogenesis, extracellular matrix expression, and expression of genes associated with osteogenesis (Heiner et al. 2006; Palomares et al. 2009; Fujisawa et al. 2018). However, increased motion between bone fragments might not always induce the upregulation of cartilaginous genes expression. A previous study reported that when small bending motions were applied to the fracture site, there was a trend toward decreased expression of chondrogenic markers during and after the stimulation period compared to rigid fixation. (Smith-Adaline et al. 2004). In the present study, quantitative RT-PCR was performed to assess the expression of *Col1a1*, *Runx2* and *Dkk1* as osteogenic markers, *Col2a1* and *Col10a1* as chondrogenic markers and *Acp5* as an osteoclastic marker. Significant differences were observed in the expression of osteogenic and chondrogenic markers between the groups, the results of quantitative RT-PCR were consistent with those of the histomorphometric and micro-CT analyses. In contrast, the expression of *Dkk1* was paradoxically increased during the fracture healing process in both groups, and there was a significant difference on day 14 between the groups. Dkk1 is secreted by osteocytes for the suppression of osteoblast function (Kim et al. 2007). The expression of *Col1a1* and *Runx2* significantly increased during fracture healing and was higher in the TiNbSn alloy group. Since Runx2 is an essential factor for osteoblast differentiation (Komori et al. 1997), the authors considered that the elevation of Runx2 induced the favorable effects for the osteogenesis in TiNbSb alloy group. Although it was paradoxical that *Dkk1* increased with the progression of ossification in the fracture callus, the authors considered the possibility that negative feedback regulation was involved where ossification was promoted, especially in the TiNbSn group. The authors speculated that these results might have been observed due to the large difference in Young's modulus between TiNbSn alloy and stainless steel. The expression of *Acp5* was significantly higher in the TiNbSn alloy group at 14 days after fracture. These findings on *Acp5* expression might indicate that osteoclast activity was increased in the TiNbSn alloy group, promoting cartilage callus resorption and bone remodeling. In a previous study, the effects of Young's moduli on fracture healing were assessed for a TiNbSn alloy (45 GPa), Ti-6Al-4V alloy (110 GPa), TiNbSn alloy (45 GPa), and annealed TiNbSn alloy (78 GPa) (Fujisawa et al. 2018; Kogure et al. 2019). Comparison between the TiNbSn alloy

(45 GPa) and the annealed TiNbSn alloy (78 GPa) demonstrated the limited differences in the results of RT-PCR analyses due to their comparatively small difference in Young's moduli (45 GPa vs. 78 GPa). In contrast, the difference in the Young's modulus between the TiNbSn alloy (45 GPa) and stainless steel (205 GPa) was large; therefore, evident differences were demonstrated in the osteogenic, chondrogenic and osteoclastic markers between the groups.

The stainless steel (SUS304) used in this study contains 18% chromium and 8% nickel, and the toxicity of nickel might have affected the process of fracture healing (Niinomi et al. 2012). New nickel-free cobalt-chromium and stainless steel materials are being developed, and future studies in comparison with such materials are expected. In this study, we employed a simple experimental system without a gyratory prevention mechanism. In a future study, the effects of the differences in Young's moduli on fracture healing should be assessed in an experimental model of intramedullary nails with a gyratory prevention and plate system for fracture treatment. Further studies in larger animals are necessary for future clinical applications. The authors have developed a hip arthroplasty stem made of TiNbSn alloy (Hanada et al. 2014) and a clinical study was performed (Approval number of ethical committee of Tohoku university hospital: #201506-1). It was confirmed that the durability, biological affinity and corrosion resistance were equivalent to those of a conventional Ti6Al4V alloy prosthesis before the clinical study. The results of the TiNbSn alloy hip prosthesis will be reported in another study. Since TiNbSn alloy has achieved safety, durability, and material availability, the final goal of the future research is to achieve clinical application of TiNbSn alloy as a fracture treatment material and shorten the fracture treatment period.

In conclusion, with the development of the new material with enhanced mechanical characteristics, an intramedullary nail with a lower Young's modulus and enough mechanical strength has been introduced. Intramedullary nails composed of a TiNbSn alloy offers an acceleration of new bone formation and fracture healing compared with stainless steel nails. TiNbSb alloy has the potential to shorten the fracture treatment period and is a promising material for orthopedic implants, including fracture treatment materials.

Acknowledgments

This work was supported by the Japan Society for the Promotion of Science (No. 18K09052 to Yu Mori).

Author Contributions

Yu Mori contributed to conceptualization, data curation, and writing original draft. Hirokazu Fujisawa contributed to data curation, writing, reviewing, and editing. Masayuki Kamimura contributed to data curation, writing, reviewing, and editing. Atsushi Kogure contributed to data curation, writing, reviewing, and editing. Hidetatsu Tanaka contributed to data curation, writing, reviewing, and editing. Naoko Mori contributed to writing, reviewing, and editing. Naoya Masahashi contributed to writing, reviewing, and editing. Toshimi Aizawa contributed to writing, reviewing, and editing. All authors approved the final version of the manuscript.

Conflict of Interest

The authors declare no conflict of interest.

References

Augat, P., Burger, J., Schorlemmer, S., Henke, T., Peraus, M. & Claes, L. (2003) Shear movement at the fracture site delays healing in a diaphyseal fracture model. *J. Orthop. Res.*, **21**, 1011-1017.

Bayraktar, H.H., Morgan, E.F., Niebur, G.L., Morris, G.E., Wong, E.K. & Keaveny, T.M. (2004) Comparison of the elastic and yield properties of human femoral trabecular and cortical bone tissue. *J. Biomech.*, **37**, 27-35.

Claes, L., Augat, P., Suger, G. & Wilke, H.J. (1997) Influence of size and stability of the osteotomy gap on the success of fracture healing. *J. Orthop. Res.*, **15**, 577-584.

Cui, C.X., Hu, B.M., Zhao, L.C. & Liu, S.J. (2011) Titanium alloy production technology, market prospects and industry development. *Mater. Des.,* **32**, 1684-1691.

Dempster, D.W., Compston, J.E., Drezner, M.K., Glorieux, F.H., Kanis, J.A., Malluche, H., Meunier, P.J., Ott, S.M., Recker, R.R. & Parfitt, A.M. (2013) Standardized nomenclature, symbols, and units for bone histomorphometry: a 2012 update of the report of the ASBMR Histomorphometry Nomenclature Committee. *J. Bone Miner. Res.*, **28**, 2-17.

Ebraheim, N.A., Martin, A., Sochacki, K.R. & Liu, J. (2013) Nonunion of distal femoral fractures: a systematic review. *Orthop. Surg.*, **5**, 46-50.

Fujisawa, H., Mori, Y., Kogure, A., Tanaka, H., Kamimura, M., Masahashi, N., Hanada, S. & Itoi, E. (2018) Effects of intramedullary nails composed of a new beta-type Ti-Nb-Sn alloy with low Young's modulus on fracture healing in mouse tibiae. *J. Biomed. Mater. Res. B Appl. Biomater.*, **106**, 2841-2848.

Glassman, A.H., Bobyn, J.D. & Tanzer, M. (2006) New femoral designs: do they influence stress shielding? *Clin. Orthop. Relat. Res.*, **453**, 64-74.

Hanada, S., Masahashi, N., Jung, T.K., Yamada, N., Yamako, G. & Itoi, E. (2014) Fabrication of a high-performance hip prosthetic stem using beta Ti-33.6Nb-4Sn. *J. Mech. Behav. Biomed. Mater.*, **30**, 140-149.

Heiner, D.E., Meyer, M.H., Frick, S.L., Kellam, J.F., Fiechtl, J. & Meyer, R.A. Jr. (2006) Gene expression during fracture healing in rats comparing intramedullary fixation to plate fixation by DNA microarray. *J. Orthop. Trauma*, **20**, 27-38.

Henderson, C.E., Kuhl, L.L., Fitzpatrick, D.C. & Marsh, J.L. (2011) Locking plates for distal femur fractures: is there a problem with fracture healing? *J. Orthop. Trauma*, **25** Suppl 1, S8-14.

Huiskes, R., Weinans, H. & van Rietbergen, B. (1992) The relationship between stress shielding and bone resorption around total hip stems and the effects of flexible materials. *Clin. Orthop. Relat. Res.*, 124-134.

Izumiyama, T., Mori, Y., Mori, S., Mori, N., Kodama, T. & Itoi, E. (2019) The effect of anti-IL-6 receptor antibody for the treatment of McH-lpr/lpr-RA1 mice that spontaneously developed destructive arthritis and enthesitis. *BMC Musculoskelet. Disord.*, **20**, 286.

Jung, T.K., Semboshi, S., Masahashi, N. & Hanada, S. (2013) Mechanical properties and microstructures of beta Ti-25Nb-11Sn ternary alloy for biomedical applications. *Mater. Sci.*

Eng. C Mater. Biol. Appl., **33**, 1629-1635.
Kamimura, M., Mori, Y., Sugahara-Tobinai, A., Takai, T. & Itoi, E. (2015) Impaired fracture healing caused by deficiency of the immunoreceptor adaptor protein DAP12. *PLoS One*, **10**, e0128210.
Khan, M.A., Williams, R.L. & Williams, D.F. (1999) The corrosion behaviour of Ti-6Al-4V, Ti-6Al-7Nb and Ti-13Nb-13Zr in protein solutions. *Biomaterials*, **20**, 631-637.
Kim, J.B., Leucht, P., Lam, K., Luppen, C., Ten Berge, D., Nusse, R. & Helms, J.A. (2007) Bone regeneration is regulated by wnt signaling. *J. Bone Miner. Res.*, **22**, 1913-1923.
Kogure, A., Mori, Y., Tanaka, H., Kamimura, M., Masahashi, N., Hanada, S. & Itoi, E. (2019) Effects of elastic intramedullary nails composed of low Young's modulus Ti-Nb-Sn alloy on healing of tibial osteotomies in rabbits. *J. Biomed. Mater. Res. B Appl. Biomater.*, **107**, 700-707.
Komori, T., Yagi, H., Nomura, S., Yamaguchi, A., Sasaki, K., Deguchi, K., Shimizu, Y., Bronson, R.T., Gao, Y.H., Inada, M., Sato, M., Okamoto, R., Kitamura, Y., Yoshiki, S. & Kishimoto, T. (1997) Targeted disruption of Cbfa1 results in a complete lack of bone formation owing to maturational arrest of osteoblasts. *Cell*, **89**, 755-764.
Kunii, T., Mori, Y., Tanaka, H., Kogure, A., Kamimura, M., Mori, N., Hanada, S., Masahashi, N. & Itoi, E. (2019) Improved osseointegration of a TiNbSn alloy with a low Young's modulus treated with anodic oxidation. *Sci. Rep.*, **9**, 13985.
Long, M. & Rack, H.J. (1998) Titanium alloys in total joint replacement - a materials science perspective. *Biomaterials*, **19**, 1621-1639.
Long, P.H. (2008) Medical devices in orthopedic applications. *Toxicol. Pathol.*, **36**, 85-91.
Maistrelli, G.L., Fornasier, V., Binnington, A., McKenzie, K., Sessa, V. & Harrington, I. (1991) Effect of stem modulus in a total hip arthroplasty model. *J. Bone Joint Surg. Br.*, **73**, 43-46.
Masahashi, N., Mori, Y., Kurishima, H., Inoue, H., Mokudai, T., Semboshi, S., Hatakeyama, M., Itoi, E. & Hanada, S. (2021) Photoactivity of an anodized biocompatible TiNbSn alloy prepared in sodium tartrate/hydrogen peroxide aqueous solution. *Appl. Surf. Sci.*, **543**.
Masahashi, N., Mori, Y., Tanaka, H., Kogure, A., Inoue, H., Ohmura, K., Kodama, Y., Nishijima, M., Itoi, E. & Hanada, S. (2017) Study of bioactivity on a TiNbSn alloy surface. *Thin Solid Films*, **639**, 22-28.
Masahashi, N., Mori, Y., Tanaka, H., Kogure, A., Inoue, H., Ohmura, K., Kodama, Y., Nishijima, M., Itoi, E. & Hanada, S. (2019) Bioactive TiNbSn alloy prepared by anodization in sulfuric acid electrolytes. *Mater. Sci. Eng. C Mater. Biol. Appl.*, **98**, 753-763.
Matsumoto, H., Watanabe, S. & Hanada, S. (2005) Beta TiNbSn alloys with low young's modulus and high strength. *Mater. Trans.*, **46**, 1070-1078.
Miura, K., Yamada, N., Hanada, S., Jung, T.K. & Itoi, E. (2011) The bone tissue compatibility of a new Ti-Nb-Sn alloy with a low Young's modulus. *Acta Biomater.*, **7**, 2320-2326.
Molster, A., Gjerdet, N.R., Raugstad, T.S., Hvidsten, K., Alho, A. & Bang, G. (1982) Effect of instability of experimental fracture healing. *Acta Orthop. Scand.*, **53**, 521-526.
Molster, A.O., Gjerdet, N.R., Alho, A. & Bang, G. (1983) Fracture healing after rigid intramedullary nailing in rats. *Acta Orthop. Scand.*, **54**, 366-373.
Mori, Y., Adams, D., Hagiwara, Y., Yoshida, R., Kamimura, M., Itoi, E. & Rowe, D.W. (2016) Identification of a progenitor cell population destined to form fracture fibrocartilage callus in Dickkopf-related protein 3-green fluorescent protein reporter mice. *J. Bone Miner. Metab.*, **34**, 606-614.
Niinomi, M. & Nakai, M. (2011) Titanium-based biomaterials for preventing stress shielding between implant devices and bone. *Int. J. Biomater.*, **2011**, 836587.
Niinomi, M., Nakai, M. & Hieda, J. (2012) Development of new metallic alloys for biomedical applications. *Acta Biomater.*, **8**, 3888-3903.
Palomares, K.T., Gleason, R.E., Mason, Z.D., Cullinane, D.M., Einhorn, T.A., Gerstenfeld, L.C. & Morgan, E.F. (2009) Mechanical stimulation alters tissue differentiation and molecular expression during bone healing. *J. Orthop. Res.*, **27**, 1123-1132.
Rack, H.J. & Qazi, J.I. (2006) Titanium alloys for biomedical applications. *Materials Science and Engineering: C,* **26**, 1269-1277.
Sha, M., Guo, Z., Fu, J., Li, J., Yuan, C.F., Shi, L. & Li, S.J. (2009) The effects of nail rigidity on fracture healing in rats with osteoporosis. *Acta Orthop.*, **80**, 135-138.
Smith-Adaline, E.A., Volkman, S.K., Ignelzi, M.A. Jr., Slade, J., Platte, S. & Goldstein, S.A. (2004) Mechanical environment alters tissue formation patterns during fracture repair. *J. Orthop. Res.*, **22**, 1079-1085.
Sumitomo, N., Noritake, K., Hattori, T., Morikawa, K., Niwa, S., Sato, K. & Niinomi, M. (2008) Experiment study on fracture fixation with low rigidity titanium alloy: plate fixation of tibia fracture model in rabbit. *J. Mater. Sci. Mater. Med.*, **19**, 1581-1586.
Tanaka, H., Mori, Y., Noro, A., Kogure, A., Kamimura, M., Yamada, N., Hanada, S., Masahashi, N. & Itoi, E. (2016) Apatite formation and biocompatibility of a low Young's modulus Ti-Nb-Sn alloy treated with anodic oxidation and hot water. *PLoS One*, **11**, e0150081.
Uhthoff, H.K., Bardos, D.I. & Liskova-Kiar, M. (1981) The advantages of titanium alloy over stainless steel plates for the internal fixation of fractures. An experimental study in dogs. *J. Bone Joint Surg. Br.*, **63-B**, 427-484.
Utvag, S.E. & Reikeras, O. (1998) Effects of nail rigidity on fracture healing. Strength and mineralisation in rat femoral bone. *Arch. Orthop. Trauma Surg.*, **118**, 7-13.
Utvag, S.E., Rindal, D.B. & Reikeras, O. (1999) Effects of torsional rigidity on fracture healing: strength and mineralization in rat femora. *J. Orthop. Trauma*, **13**, 212-219.